JOURNAL OF MATERIALS SCIENCE **40** (2005) 367–371

Measurement of effective nugget by thermoelastic stress in spot weldments

JOONHYUK SONG
Department of Mechanical and Aerospace Engineering, Chonbuk National University, South Korea
E-mail: songjh33@chonbuk.ac.kr

A. SHIMAMOTO
Department of Mechanical Engineering, Saitama Institute of Technology, Japan

HYOSUN YU, HEEYONG KANG, SUNGMO YANG
Department of Mechanical and Aerospace Engineering, Chonbuk National University, South Korea
E-mail: yangsm@chonbuk.ac.kr

Spot welding process is completed in very short time and there are many factors affecting on the generation of welding defects. There are difficult to control experimental factors. Even more this is hard to monitor of distribution stress in practical cases. And too much time and expense are required for the experimental trials to find the proper welding condition. The purpose of this study is to investigate the applicability of infrared thermagraphy for the evaluation of weldability in spot weldment. There are some problems in the destructive methods. Furthermore, it is very complicated to apply it on actual structure because of time and cost consuming. Therefore, a nondestructive method for estimating the nugget size has been in continual demand. In this study, thermoelastic stress analysis adopting an infrared thermography for nondestructive evaluation of spot weldability is investigated. Using temperature and stress distribution obtained by infrared camera from adiabatic heat expansion under a repeated load of sinusoidal waves, we estimated the effective nugget of spot welded specimens. To examine the evaluated effective nugget size in spot weldments, they have been compared with the results of microstructure observation from a 5% Nital etching test.

1. Introduction

Spot welding is one of the important welding processes for the construction of thin metal sheet. Because of low investment cost, alternating welding current is widely applied for power source. Direct current type could be used for high quality weldment. However, spot weldments, which are welded by a point phase of several millimeters, are the main cause of fatigue crack since they are strongly influenced by a repeated load due to a structural deformation, residual stress, stress concentration, and a like. Particularly, the fatigue cracks caused by repeated external load are concentrated on the spot weldments in a dynamic structure such as an automobile [1, 2].

The evaluation of fatigue strength of spot weldments is complicated since fatigue strength is influenced by various factors, including geometric shape, pressure, residual stress, material, etc. The strength in a thin plate depends heavily on the extent of the stress concentration around the nugget but relatively small on the residual stress deteriorated by a repeated load or a reduction of fatigue stress. Therefore, an evaluation on the nugget size of the weldment is important [3–5].

The nugget size and the welding of the spot weldments, which are used in the parts of sheet metals in an automobile are evaluated entirely by destructive tests, that is experimental methods including peel test relating to joint strength, tensile-diagnosis test, and cross tensile test.

Welding strength of spot weldment have been investigated by a number of peel tests in the manufacturing fields at automobile factories. It is very difficult to apply in a real weldment or a weldment with a complicate shape in a practical manufacturing process. But the traditional welding conditions based on tensile strength require many numbers of iterative tests [6, 7].

Recently, an evaluation method for spot welding strength using a finite element method or mathematical method were studied [8–11]. A nugget size could be defined by an observation on cut-off surface of specimen using a microscope.

For the spot weldments with uncoated cold rolled steel plates (SPC), which are widely used in

automobiles, the effective nugget was measured by the thermoelastic stress measuring method. The feasibility of the estimated effective nugget was examined by comparing with the cut-off surfaces made by 5% Nital etching test after a fatigue test.

2. Experimental procedure

The thermoelastic stress measurement is based on the principle that when a solid is compressed, it is heated slightly. When the pressure on it is released, it returns to its original shape (elasticity) and its original temperature (thermoelasticity). The temperature of a solid in terms of the change in the sum of the principal stresses is

$$\Delta T = (-kT\Delta\sigma)/\rho C_{\mathrm{v}} = -K_{\mathrm{m}} T \Delta\sigma \quad (1)$$

where k, heat expansion coefficient; T, ambient temperature; ρ, density; C_{v}, specific heat at constant volume; K_{m} heat elastic modulus; and σ_{IR} stress by infrared thermography.

When a stress is lower than an elastic limit, the following equation is made between the varied amount of temperatures ΔT and the varied amount of principal stresses $\Delta\sigma$. It makes us possible to measure a change of main stresses by measure a change of temperatures, as well.

The equation assumes adiabatic conditions (no significant heat loss). As a practical matter, the adiabatic assumption is met by continually and 'rapidly' changing the load on the structure. Heat loss by conduction (a non-adiabatic condition) only becomes an issue in the case of high thermal gradients. For instance, a small aluminum structure would be a case where special attention to the adiabatic assumption is important. It is clear that significant convective or radiant heat loss is not common.

Measurement time must be balanced with temperature resolution. Because of the statistical nature of the measurement, image-averaging techniques are used to improve the stress resolution. The inverse square rule that applies to most noise limited measurements describes this trade-off. Improving the stress resolution by a factor of two lengthens the measurement time by a factor of four.

The test was done by using SPC lap joint whose chemical compositions and mechanical properties as shown in Table I and Fig. 1. Tensile-shear specimens are prepared by two pieces of uncoated SPC plates(100 mm × 30 mm × 1.0 mm), which are lapped 30 mm and one point spot welded.

Welding conditions were adopted in Table II. The electrodes of R shape (dome type) with aluminum oxide or dispersed reinforced copper were used in the point welding whose range conformed to $5\sqrt{t}$ recommended by the RWMA class II for the thickness of welding parts.

Specimen was vibrated to a constant frequency by a repeated load of 980 N using a fatigue tester for the spot welding specimens as shown in Fig. 2. Simultaneously,

TABLE I Chemical compositions and mechanical properties of the base metals

C	Si	Mn	P	S	Ni	Al
(a) Chemical compositions (Fe bal. %)						
4.3	1.9	42.4	7.9	0.7	2.6	4.7

Tensile strength (MPa)	Elongation (%)	Young's modulus (GPa)	Possion's ratio (ν)
(b) Mechanical properties			
296.84	56	194	0.3

TABLE II Welding conditions

Welding current (kA)	Electrode force (MPa)	Squeeze time (cycle)	Welding time (cycle)	Holding time (s)
8	250	30	15	10

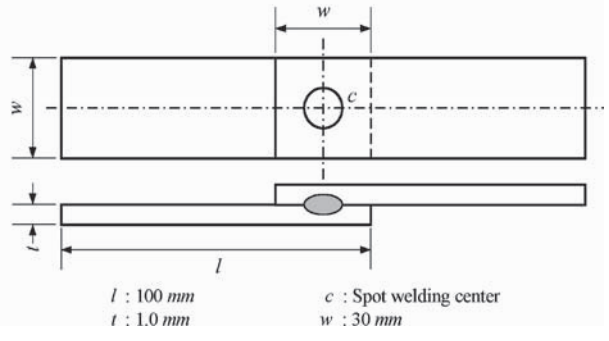

Figure 1 Specimen of spot weldments.

stress of spot weldment was measured by measuring a varied amount of temperatures at the point of weldments using a infrared camera (DELTA THERM TSA 1000). The process was as follows.

(1) *Thermoelastic stress measured by the vibrating frequency of load*. Since the IR stress (analyzed thermoelastic stress from the infrared camera) is dependent on the vibrating frequency, a stress was measured by changing the frequency by from 4 to 20 Hz to acquire a vibrating frequency for the experiment.

(2) *Correlation between temperature and stress*. Dividing the spot welded specimen into 2 parts lengthwise as shown in Fig. 3, temperature on one side were measured by a 3 axes strain gauge, and then the correlation between temperature-stress was conducted.

(3) *Evaluation of the effective nugget*. The effective nugget was evaluated from the stress distribution diagram around the hot spot of specimen by adding up the measured temperatures obtained from the infrared camera.

A correlation between temperature changes and stresses from an infrared camera was obtained by traditional measurement of strain of the specimens with a strain gauge as shown in Fig. 3. The experiment was done by a load control method that uses a hydraulic dynamic fatigue tester with capacity of 10 ton at 10 Hz and stress ratio $R \approx 0$.

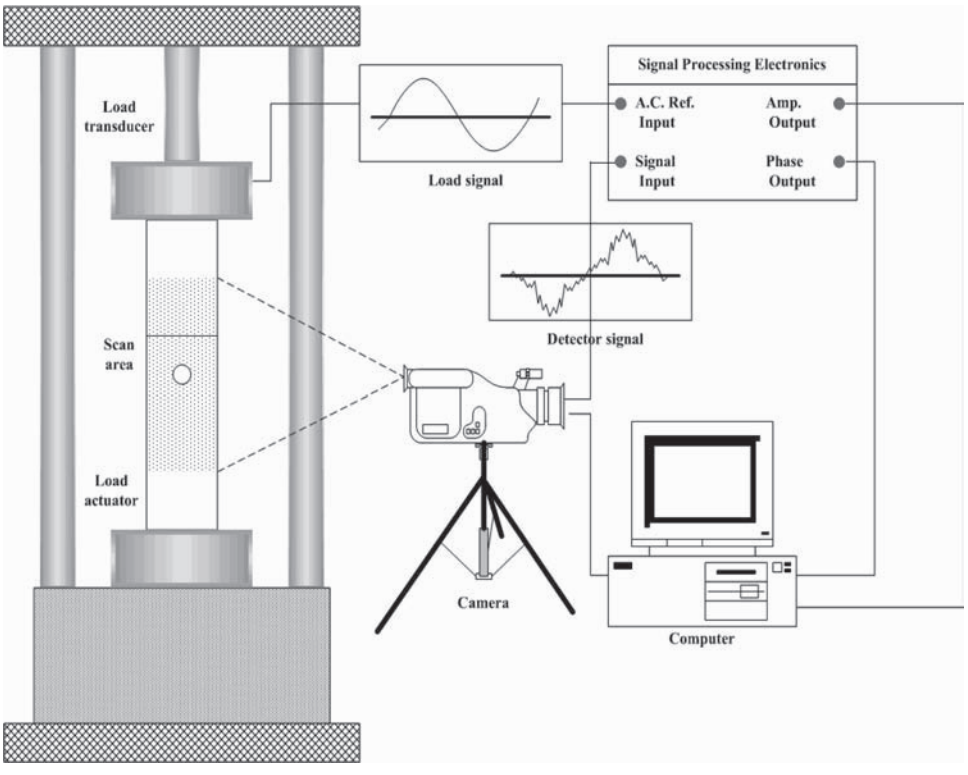

Figure 2 Thermoelastic stress measurement with infrared camera system.

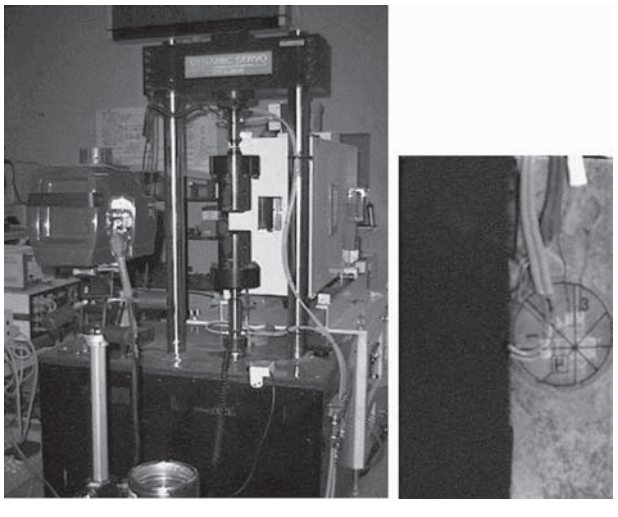

Figure 3 Stress measurement with infrared stress analysis system and strain gauge for the temperature-stress equation.

In fact, it is important that the surface of the structure being measured be an efficient and diffuse emitter of infrared radiation. This is accomplished by preparing the surface with a flat black paint as shown in Fig. 3.

To increase the accuracy and repeatability of the measurements, the temperature changes induced by the thermoelastic effect are repeated and time-averaged during continuous dynamic loading.

The effect of loading frequency on the physical and instrumentation systems is complex. However, there is no compensation for frequency effects is available as a general because specimens are various and complex.

To get a loading frequency, infrared stresses were measured with vary loading frequencies from 4 to 20 Hz.

Finally, to examine the effective nugget by thermoelastic stress with an infrared camera, we observed the cut-off surfaces of the same kind of specimens using a microscope. After cutting off the spot weldment at the center of the surface perpendicularly, those surfaces were polished with an emery paper and then etched with 5% Nital etching liquid for 20 s. And the size of nugget was measured by an optical microscope.

3. Results and discussion

Stress of spot weldment was measure by the thermoelastic stress measurement system. And with this result, the effective nugget of the spot weldment was evaluated and compared with that obtained with an optical microscope.

Temperature distribution was measured by an infrared camera. A sinusoidal wave load of 10 Hz was applied on the specimens. Fig. 4 shows the experimental results on loading frequency and IR stress. Infrared

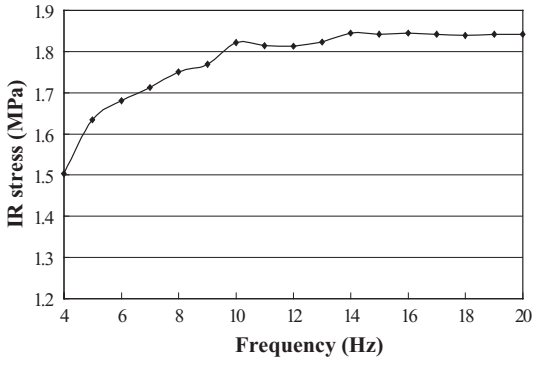

Figure 4 IR stress vs. loading frequency.

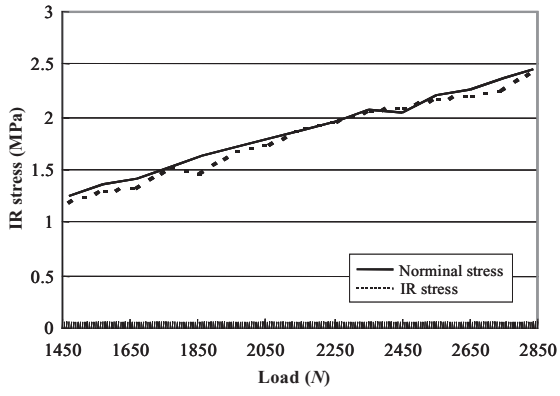

Figure 5 IR stress compared to the nominal stress.

thermography showed that the temperature varied with the change of the loading frequency. Since measured thermoelastic stresses were not linear, when the loading frequencies were lower than 10 Hz. Therefore, a loading frequency of 10 Hz was used for the experiment since the IR stresses from the thermoelastic stress measurement method by infra-red camera become almost constant when the vibra-ting frequency is greater than 10 Hz.

A stress distribution is calculated by amplifying and filtering the amounts of temperature changes, obtained from the output terminal. The relationship between the temperature changes and the stresses during that the load was varied from 1450 to 2850 N as shown in Fig. 5.

From the graph, the IR stress σ_{IR} is as follows.

$$\sigma_{IR} = 9.5 \times 10^5 + 120\Delta T \qquad (2)$$

In this study, the IR stress equation is linear as shown above because the structure is a simple tensile-shear test specimen. However, in practical cases, the IR stress equation would be more complex or nonlinear, a topic which would be studied in our future research.

Obtained by infrared camera, the temperature distribution around HAZ (heat affected zone) of the spot weldment is shown in Fig. 6. It is the nugget in circle at center. Upward from center, it is tensile stress distribution of loading-direction from nugget. Downward from center, it is compression stress distribution of outer-direction from nugget.

Stress distribution around HAZ is derived after transferring the stresses from the Equation 2 in Fig. 7. Since a

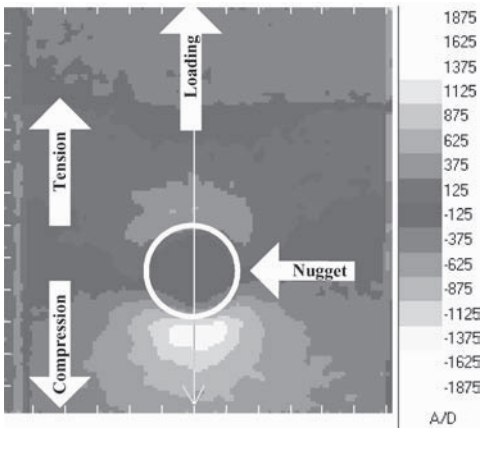

Figure 6 Infrared thermography.

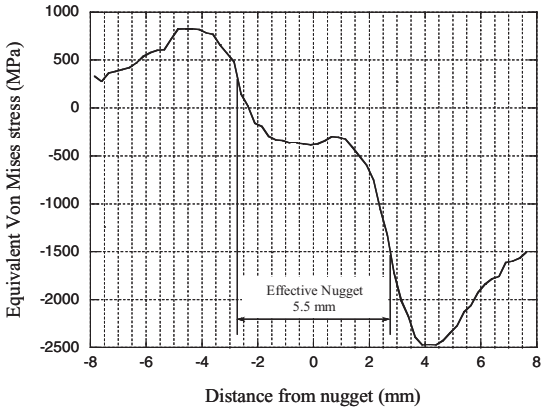

Figure 7 Stress distribution around the spot welding points and the effective nugget size.

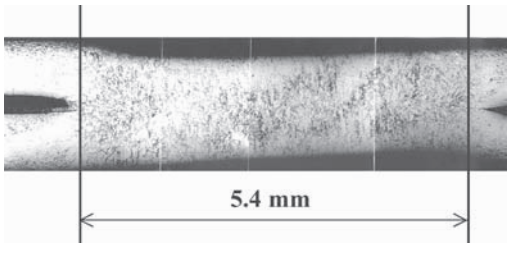

Figure 8 Nugget size of the spot weldment by a microstructure observation.

particle size of a nugget varies with the material, the gradient of stress was the changes as point of contraflexuer. This makes us possible to confirm the intercepting point that varies from a stress ingredient of the body material to that of the nugget part. A distance between the incepting points is defined to be an effective nugget. Effective nugget around the SP(spot point) has been evaluated to be 5.5 mm, based on the stress distribution .

From Fig. 8, the size of nugget is 5.4 mm, measured using an optical microscope of the cut-off surface. The effective nugget size, 5.5 mm, which was measured by the thermoelastic stress analysis, agrees well with the nugget size of 5.4 mm when observed with an optical microscope.

4. Conclusion

In this study, the effective nugget size of spot weldments with uncoated cold rolled steel plate was measured by the thermoelastic stress analysis and examined by comparing it with the results obtained from optical microscope observations of the cut-off surface with 5% Nital etching test. Temperature and stress relationship was derived from both the measurements of the temperature distribution, obtained using an infrared camera, and the stresses obtained using a strain gauge.

The conclusions are as follows:

(1) Thermoelastic stress shall be measured at a vibrating frequency of more than 10 Hz since the stress depends on the frequency.

(2) The effective nugget of the spot weldment would be measured using a point of contraflexuer

of stress distribution with thermoelastic stress measurement.

Our study presented an measurement procedure for the effective nuggets of spot weldments, that uses a non-destructive method. In our future study, the usefulness of this procedure for monitoring the health of a structure in practical process of automobile manufacturing will be examined.

References

1. C. M. SUH and S. S. KANG, *J. Korean Soc. Mech. Eng.* **12**(4) (1988) 747.
2. H. S. YU, *ibid.* **13**(11) (1999) 775.
3. B. POLLARD, SAE 820284 (1982).
4. F. V. LAWRENCE, SAE 830035 (1983).
5. M. FARID, *J. Mater. Sci.* **35**(15) (2000) 3817.
6. D. J. VANDENBOSSCHE, SAE 770214 (1977) p.1.
7. M. SUZANNE, SAE 850273 (1985) p.1.
8. T. S. LEE, H. Y. LEE and S. J. SHIN, *J. Korean Soc. Autom. Eng.* **6**(6) (1998) 40.
9. A. OTHMANI, *J. Mater. Sci.* **34**(20) (1999) 5139.
10. G. J. HAN, H. Y. JEON and H. C. LEE, *J. Korean Soc Autom. Eng.* **8**(6) (2000) 173.
11. I. S. SOHN and D. H. BAE, *ibid.* **8**(3) (2000) 110.

Received 27 August 2003
and accepted 29 April 2004